Harris, D. A. (1978) *Biochim. Biophys. Acta 463*, 245-273.
Harris, D. A., & Baltscheffsky, M. (1979) *Biochem. Biophys. Res. Commun. 86*, 1248-1255.
Harris, D. A., Dall-Larsen, T., & Klungsoyr, L. (1981) *Biochim. Biophys. Acta 635*, 412-428.
Hochman, Y., & Carmeli, C. (1981) *Biochemistry 20*, 6287-6292.
Kohlbrenner, W. E., & Boyer, P. D. (1983) *J. Biol. Chem. 258*, 10881-10886.
Leckband, D., & Hammes, G. G. (1987) *Biochemistry 26*, 2306-2311.
Lien, S., & Racker, E. (1971) *Methods Enzymol. 23*, 547-555.
Lunardi, J., Gerin, J., Issartel, J.-P., & Vignais, P. V. (1987) *J. Biol. Chem. 262*, 15172-15181.
Magnusson, R. P., & McCarty, R. E. (1976) *J. Biol. Chem. 251*, 7417-7422.
Malyan, A. N. (1981) *Photosynthetica 15*, 474-483.
Malyan, A. N., & Vitseva, O. I. (1983) *Photosynthetica 17*, 499-505.
Melese, T., & Boyer, P. D. (1985) *J. Biol. Chem. 260*, 15398-15401.
Milgrom, Ya. M., & Murataliev, M. B. (1986) *Biol. Membr. 3*, 781-791.
O'Neal, C. C., & Boyer, P. D. (1984) *J. Biol. Chem. 259*, 5761-5767.
Penefsky, H. S. (1979) *Adv. Enzymol. Relat. Areas Mol. Biol. 49*, 224-280.
Rosen, G., Gresser, M. J., Vinkler, C., & Boyer, P. D. (1979) *J. Biol. Chem. 254*, 10654-10661.
Schlodder, E., & Witt, H. T. (1981) *Biochim. Biophys. Acta 635*, 571-584.
Schumann, J. (1987) *Biochim. Biophys. Acta 890*, 326-334.
Shavit, N., & Strotmann, H. (1980) *Methods Enzymol. 69*, 323-326.
Shoshan, V., & Selman, B. R. (1979) *J. Biol. Chem. 254*, 8801-8807.
Smith, D. J., & Boyer, P. D. (1976) *Proc. Natl. Acad. Sci. U.S.A. 73*, 4314-4318.
Smith, L. T., Rosen, G., & Boyer, P. D. (1983) *J. Biol. Chem. 258*, 10887-10894.
Strotmann, H., & Bickel-Sandkötter, S. (1977) *Biochim. Biophys. Acta 460*, 126-135.
Strotmann, H., Hese, H., & Edelman, K. (1973) *Biochim. Biophys. Acta 314*, 202-210.
Strotmann, H., Bickel, S., & Huchzermeyer, B. (1976) *FEBS Lett. 61*, 194-198.
Strotmann, H., Kleefeld, S., & Lohse, D. (1987) *FEBS Lett. 221*, 265-269.
Thomassen, J., & Klungsoyr, L. (1983) *Biochim. Biophys. Acta 723*, 114-122.
Vasilyeva, E. A., Minkov, I. B., Fitin, A. F., & Vinogradov, A. D. (1982) *Biochem. J. 202*, 15-23.
Wise, J. G., Hicke, B. J., & Boyer, P. D. (1987) *FEBS Lett. 223*, 395-401.
Wu, D., & Boyer, P. D. (1986) *Biochemistry 25*, 3390-3396.
Xue, Z., Zhou, J.-M., Melese, T., Cross, R. L., & Boyer, P. D. (1987a) *Biochemistry 26*, 3749-3753.
Xue, Z., Miller, C. G., Zhou, J.-M., & Boyer, P. D. (1987b) *FEBS Lett. 223*, 391-394.

NMR Signal Assignments of Amide Protons in the α-Helical Domains of Staphylococcal Nuclease

Dennis A. Torchia,*,‡ Steven W. Sparks,‡ and Ad Bax§

Bone Research Branch, National Institute of Dental Research, and Laboratory of Chemical Physics, National Institute of Diabetes and Digestive and Kidney Diseases, National Institutes of Health, Bethesda, Maryland 20892

Received February 16, 1988; Revised Manuscript Received May 5, 1988

ABSTRACT: We report complete assignments of the amide proton signals in the three long d_{NN} connectivity sequences observed in the NOESY spectrum of deuteriated staphylococcal nuclease (Nase) complexed with thymidine 3',5'-bisphosphate (pdTp) and Ca^{2+}, M_r 18K. The assignments are made by comparing NOESY spectra with ^1H-^{15}N and ^1H-^{13}C heteronuclear multiple-quantum shift correlation (HMQC) spectra of Nase samples containing ^{15}N- and ^{13}C-labeled amino acids. The assignments show that the residues which are linked by the d_{NN} connectivity sequences are located in the three α-helical domains of Nase. Our results indicate that by combining NOESY and HMQC spectra of appropriately labeled samples it should be possible to delineate and study α-helical domains in soluble proteins having molecular weights that are greater than 18K.

Staphylococcal nuclease, Nase,[1] is a well-characterized enzyme that has been the subject of many structure–function studies (Tucker et al., 1978, 1979a,b,c). The recent success in expressing the structural gene of Nase in *Escherichia coli* (Shortle, 1983) has generated much new interest in understanding the activity and structure of the protein (Calderon et al., 1985; Shortle & Lin, 1985; Fox et al., 1986; Evans et al., 1987; Hibler et al., 1987; Serpersu et al., 1987). Although two-dimensional proton nuclear magnetic resonance, NMR, spectroscopy is a powerful method for determining the solution structures of small proteins (Wuethrich, 1986), spectra of

‡ Bone Research Branch.
§ Laboratory of Chemical Physics.

[1] Abbreviations: Nase, staphylococcal nuclease; pdTp, thymidine 3',5'-bisphosphate; NMR, nuclear magnetic resonance; NOE, nuclear Overhauser effect; NOESY, two-dimensional NOE spectroscopy; HMQC, two-dimensional heteronuclear multiple-quantum shift correlation spectroscopy.

proteins the size of Nase are difficult to interpret because of overlap of broad resonances and because of spin diffusion. Recently we have deuteriated the nonexchangeable hydrogens of Nase to overcome these problems (Torchia et al., 1988) and have observed many d_{NN} connectivities with high sensitivity in the NOESY spectrum of deuteriated Nase complexed with pdTp and Ca^{2+}, M_r 18K. In a recent related application, LeMaster and Richards (1988) have reported the sequential assignment of randomly deuteriated thioredoxin, an enzyme with M_r 11.7K.

Of particular interest in the NOESY spectrum of deuteriated Nase was the observation of three long sequences of d_{NN} connectivities, because these sequences are indicative of helical domains (Zuiderweg et al., 1983; Williamson et al., 1984; Clore et al., 1985; Wand & Englander, 1985; Weber et al., 1985; Klevit & Drobny, 1986; Wuethrich, 1986). Herein we use heteronuclear multiple-quantum shift correlation, HMQC, spectroscopy (Mueller, 1979; Bax et al., 1983; Bendal et al., 1983; Griffey & Redfield, 1987) of 1-$^{13}C/^{15}N$ double-labeled samples to edit (LeMaster & Richards, 1985; Griffey et al., 1985) and to sequentially assign (Kainosho & Tsuji, 1982; Griffey et al., 1986; McIntosh et al., 1987, 1988; Senn et al., 1987) the amide proton signals, linked by the long sequences of d_{NN} connectivities, to residues in the α-helical domains of Nase. We also assign other proton and amide ^{15}N signals. These assignments provide numerous starting points for additional assignments of Nase signals, and more significantly, they allow one to examine the effects of important quantities such as site mutations, ligand interactions, solvent conditions, etc. upon the structure of the helical domains of Nase.

Experimental Procedures

Nase was obtained from *Escherichia coli* (provided by Professor John Gerlt) grown in defined media, following procedures (Hibler et al., 1987) for labeling and purifying the protein. With two exceptions, scrambling of the labels was not observed. Samples labeled with [^{15}N]E were equally well labeled with [^{15}N]Q, and samples labeled with [^{15}N]S were labeled 30–40% as well with [^{15}N]G. Due to the construction of the expression vector, the sample obtained has a heptapeptide (M-D-P-T-V-Y-S) appended to the N-terminus of the protein. The extension does not affect enzyme activity or stability (Calderon et al., 1985). ^1H–^{15}N HMQC spectra were obtained on solutions having the following compositions: H_2O, 90%; ^2H_2O, 10%; NaCl, 100 mM; Nase, 1.5–1.8 mM; pdTp, 5 mM; $CaCl_2$, 10 mM; borate buffer, pH 7.7, 50 mM. The pH meter readings of the Nase solution were in the range 7.3–7.6. Spectra of several samples were recorded at pH 7.0 and 7.5; within experimental uncertainty (see below) the observed chemical shifts were the same at the two pH values. ^1H–^{13}C HMQC RELAY spectra (Lerner & Bax, 1986) were recorded in the same solvent system except that 99.996% ^2H_2O was used.

All spectra were recorded on a modified NT 500 spectrometer in the absorption mode by use of published pulse sequences (Lerner & Bax, 1986; Sklenar & Bax, 1987) with the following settings: 90° pulses, ^1H/30 μs, ^{13}C/100 μs, ^{15}N/250 μs; recycle delay, 0.7 s; acquisition time, 0.05 s; spectral windows, ^1H/14.8 ppm, ^{13}C/50 ppm, ^{15}N/25–50 ppm; 64–512 scans per t_1 value; 64–192 t_1 values; 36.5 °C. ^1H–^{15}N spectra were normally recorded with a 1–1 echo to minimize excitation of the H_2O signal (Redfield, 1983; Griffey et al., 1985; Sklenar & Bax, 1987). In a few cases spectra were also obtained with saturation of the H_2O signal. The spectrometer settings used to record the NOESY spectra of the deuteriated protein are given by Torchia et al. (1988). Proton chemical shifts are relative to the water signal at δ 4.65 in ^2H_2O and at δ 4.67 in H_2O at 36.5 °C. ^{15}N and ^{13}C chemical shifts are relative to external ammonia and TSP (Merck), respectively. Signal frequencies were measured with the Nicolet peak pick software. Uncertainties in chemical shifts are 0.02 and 0.1 ppm for protons and heteronuclei, respectively.

Table I: Chemical Shifts[a] and Assignments of Nase Amide Protons in the Three d_{NN} Sequences

a sequence		b sequence		c sequence	
δ_H	assignment	δ_H	assignment	δ_H	assignment
8.88	a1, A58	9.65	b1, N100	8.08	c1, L125
8.29	a2, S59	6.19	b2, E101	8.90	c2, R126
8.38	a3, A60	7.83	b3, A102	7.98	c3, K127
8.09	a4, F61	7.95	b4, L103	7.60	c4, S128
8.60	a5, T62	6.88	b5, V104	8.44	c5, E129
8.06	a6, K63	9.12	b6, R105	7.94	c6, A130
7.90	a7, K64	7.09	b7, Q106	7.44	c7, Q131
7.64	a8, M65	8.02	b8, G107	7.85	c8, A132
8.29	a9, V66			8.14	c9, K133
8.77	a10, E67			7.76	c10, K134
7.33	a11, N68			7.62	c11, E135
6.69	a12, A69			7.80	c12, K136
				7.57	c13, L137

[a] From NOESY spectra of deuteriated Nase (Torchia et al., 1988).

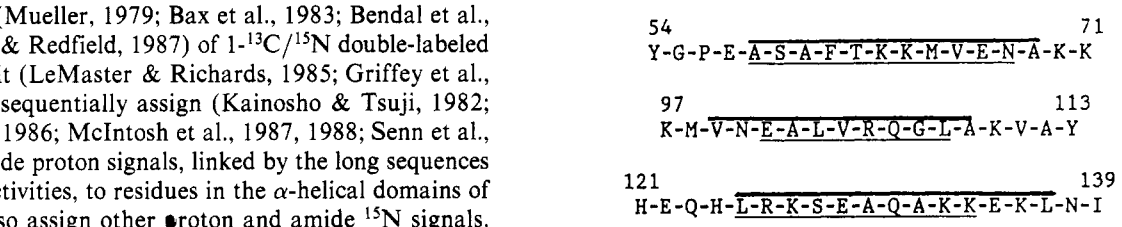

FIGURE 1: Portions of the amino acid sequence of Nase (Tucker et al., 1978) that encompass the three α-helical domains (Tucker et al., 1979b) of the protein. The backbone amide proton of each underlined residue is hydrogen bonded to a carbonyl oxygen four residues away. The overlined residues are those assigned to the sequences of d_{NN} connectivities as described in the text.

Results

The three long sequences of d_{NN} connectivities identified in the NOESY spectra of deuteriated Nase (Torchia et al., 1988) are designated a, b, and c, respectively. The amide proton signals connected in each sequence are designated a1–a12, b1–b8, and c1–c13, and their chemical shifts, δ_H, are listed in Table I. In order to assign the signals in the d_{NN} connectivity sequences, we have obtained ^1H–^{15}N HMQC spectra of Nase containing one type of amino acid labeled with α-^{15}N and a second type of amino acid labeled with 1-^{13}C, permitting immediate identification of unique dipeptide sequences that were double-labeled (Kainosho & Tsuji, 1982; Cross & Opella, 1985; Griffey et al., 1986; Leighton & Lu, 1987; McIntosh et al., 1987). Because long sequences of d_{NN} connectivities are signatures of helical structures, labeled amino acids chosen for incorporation into Nase were those located either within or adjacent to one of the α-helical domains in the protein (Tucker et al., 1979b). The chemical shifts derived from the HMQC spectra are listed in Table II. We now show that a unique set of assignments of all signals in the three d_{NN} connectivity sequences is obtained by comparing the data in the two tables.

Assignments of the Signals in the a Sequence of d_{NN} Connectivities. Examination of Figure 1 shows that F61 and M65 are in the same helical domain and that the other helical domains are devoid of these residues. We therefore obtained HMQC spectra of Nase labeled with [^{15}N]Phe and [^{15}N]Met in order to assign the d_{NN} connectivity sequence that contains

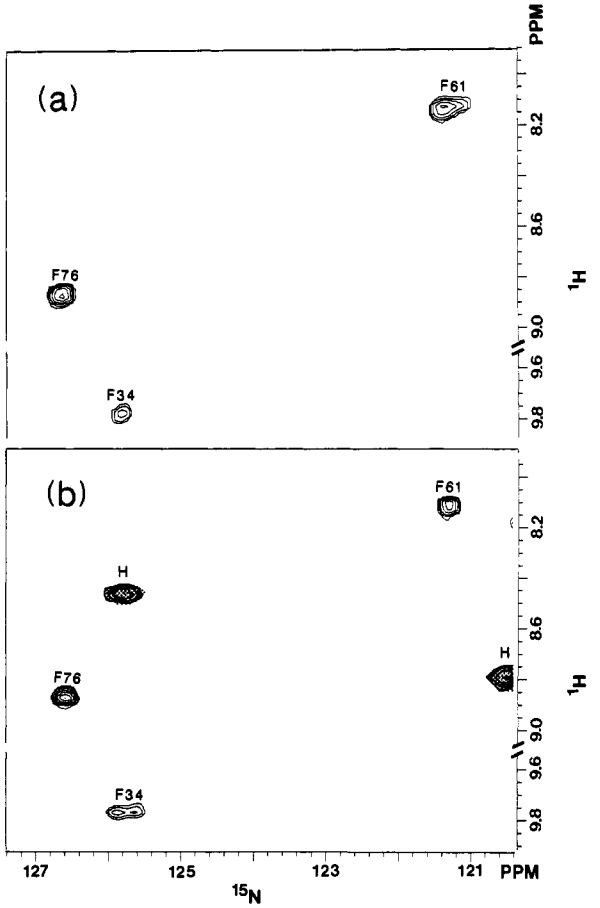

FIGURE 2: Comparison of ^{1}H–^{15}N HMQC spectra of Nase labeled with (a) [1-^{13}C]A/[^{15}N]F and (b) [1-^{13}C]T/[^{15}N]F/[^{15}N]H. The signal assignments given in these and subsequent spectra are discussed in the text. The shaded signals in (b) are due to His residues.

signals of these residues. One must assign at least two signals in a d_{NN} connectivity sequence to ensure that the direction of the sequential assignment is correct.

Assignments of the signals of the three Phe amide protons and nitrogens in Nase, Table II, are obtained from the HMQC spectra of Nase labeled with [1-^{13}C]A/[^{15}N]F, Figure 2a, and [1-^{13}C]T/[^{15}N]F/[^{15}N]H, Figure 2b. The scalar coupling of T33-F34 splits the signal at δ_H 9.74, which is therefore assigned to F34. Because the level of Ala ^{13}C enrichment in Nase, 40–50%, is only half that of Thr, none of the three Phe signals in Figure 2a shows a clear splitting. However, the signal at δ_H 8.11 is broader, along the nitrogen chemical shift axis, than the other two Phe signals and is significantly broader than the corresponding signal in Figure 2b. These observations show that broadening of the signal at δ_H 8.11 in Figure 1a is due to A60-F61 ^{13}C–^{15}N scalar coupling, and therefore, this signal is assigned to F61. The remaining signal at δ_H 8.85 is assigned to F76.

Comparison of Tables I and II shows that F61 can be assigned to a4, c1, or c9. In order to distinguish among these possible assignments, HMQC spectra of Nase labeled with [1-^{13}C]L/[^{15}N]M, Figure 3a, and [1-^{13}C]K/[^{15}N]M, Figure 3b, were obtained. Signals of the four Met amide protons in Nase are observed in each spectrum. The HMQC signal at δ_H,δ_N 9.56,122.0 is split, Figure 3b, by the L25-M26 scalar coupling and is therefore assigned to M26. Although the K–M peptide bond occurs twice in the Nase sequence, K64-M65 and K97-M98 (Tucker et al., 1978), only the signal at δ_H 7.67 is clearly split into a doublet. Because this is the only Met signal whose proton chemical shift matches any of the proton

Table II: Chemical Shifts[a] and Assignments of Backbone Amide Protons and Nitrogens in Nase

residue	δ_H	δ_N	assignment	residue	δ_H	δ_N	assignment
His	6.82	113.3	H121	Val	6.89	117.0	V104
	8.15	120.2			6.99	103.8	V39
	8.44	125.8			7.76	121.5	
	8.76	120.5			7.82	119.4	
Leu	7.49	121.9			7.97	122.5	
	7.58	117.0	L137		8.28	107.8	V66
	7.80	115.3	L108		9.15	120.7	
	7.95	115.5	L103		9.28	124.0	
	8.07	118.1	L125		9.52	117.2	
	8.24	122.1	L7/L25		10.18	136.1	V99
	8.27	126.1		Glx[b]	6.19	112.7	E101
	8.31	124.8			7.10	112.1	Q106
	9.15	125.1			7.43	118.2	Q131
	9.35	127.2	L7/L25		7.55	120.3	
	9.38	111.7			7.63	116.5	E135
Met	7.67	116.2	M65		7.81	124.7	
	9.23	126.6	M98		7.83	119.3	
	9.56	122.0	M26		7.90	121.2	
	9.57	125.8	M32		8.22	126.9	E52/E75[c]
Phe	8.11	121.3	F61		8.31	119.1	
	8.85	126.6	F76		8.32	121.3	
	9.74	125.8	F34		8.45	125.0	E129
Ser[b]	7.58	117.9	S128		8.74	124.8	
	7.84	119.4			8.78	121.1	E67
	8.09	116.1	S141		8.80	123.3	
	8.32	111.7	S59		8.84	126.8	E52/E75[c]

[a] From ^{1}H–^{15}N HMQC spectra. [b] Signals of two Ser and two Glx residues were not seen in the HMQC spectra, presumably because of rapid hydrogen exchange. [c] From splitting by [1-^{13}C]V.

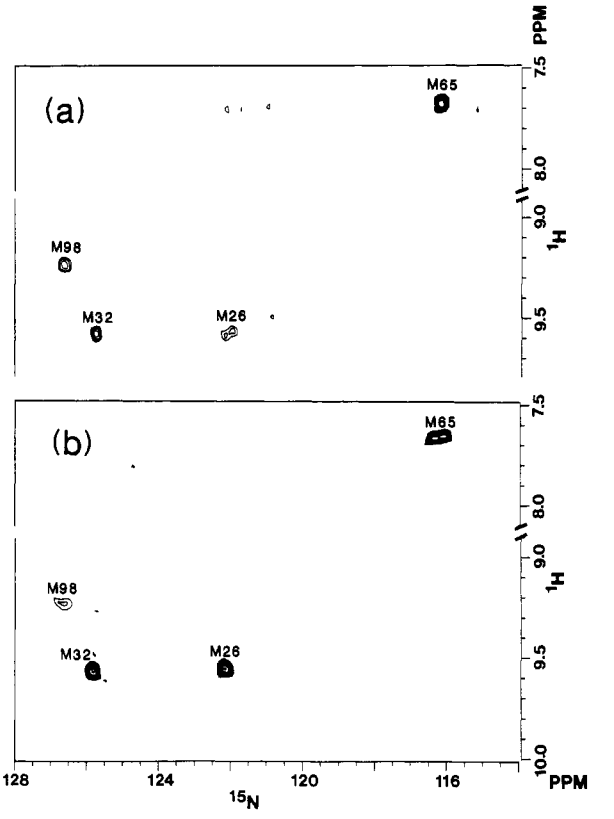

FIGURE 3: Comparison of ^{1}H–^{15}N HMQC spectra of Nase labeled with (a) [1-^{13}C]L/[^{15}N]M and (b) [1-^{13}C]K/[^{15}N]M.

shifts in the d_{NN} connectivity sequences, it is assigned to M65. Comparison of the signal at δ_H 9.23 in panels a and b of Figure 3 shows that this signal is strongly perturbed by the ^{13}C–^{15}N coupling, and it is therefore assigned to M98. This signal is broad and has small relative intensity even when coupling is absent, Figure 3a, presumably as a consequence of exchange

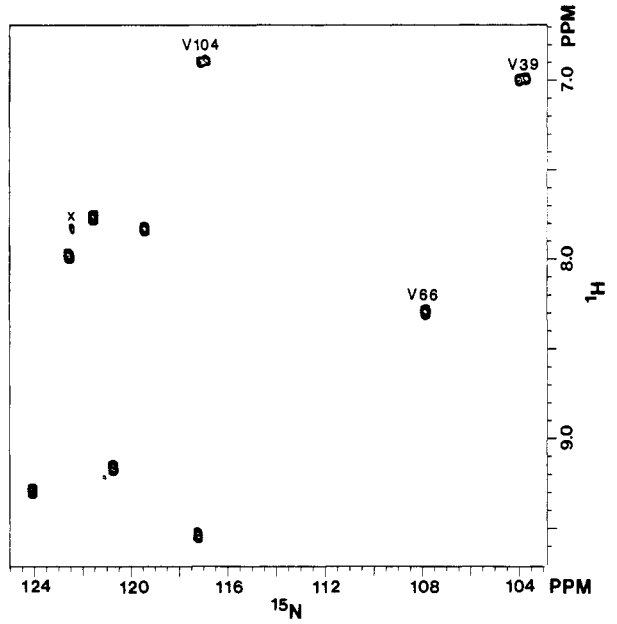

FIGURE 4: ^{1}H–^{15}N HMQC spectrum of Nase labeled with [1-^{13}C]-L/[^{15}N]V. One Val signal at δ_H,δ_N 10.18,136.1 lies outside the portion of the spectrum shown. The weak signal indicated by the x has not been identified.

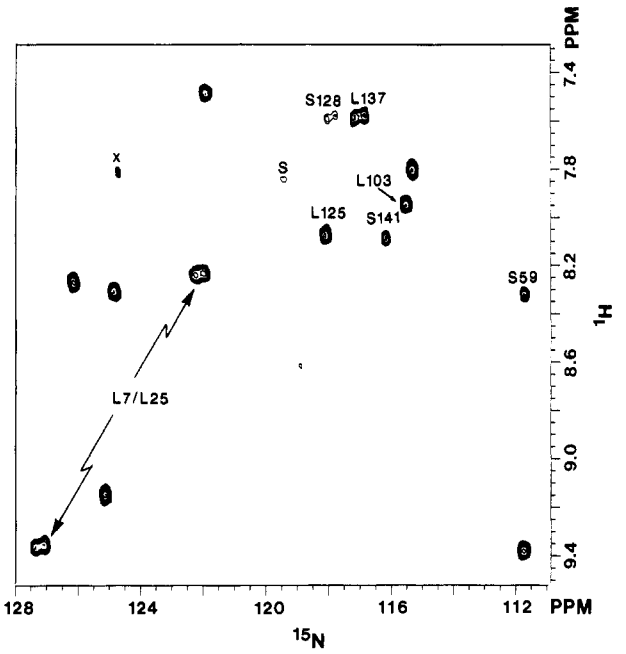

FIGURE 5: ^{1}H–^{15}N HMQC spectrum of Nase labeled with [1-^{13}C]-K/[^{15}N]L/[^{15}N]S. The Leu and Ser signals were identified in spectra of Nase samples which contained either [^{15}N]L or [1-^{13}C]W/[^{15}N]S. The spectrum of the latter sample (not shown) shows a split signal at δ_H 8.09 which is assigned to S141 because W140 is the only Trp in Nase. The Leu signals are significantly more intense than the Ser signals because labeled Leu incorporates into Nase with greater efficency than labeled Ser. The weak signal indicated by the x has not been identified.

of the amide proton of M98 with water. We think that exchange broadening is responsible for the lack of a clear splitting in the HMQC spectrum. The only HMQC signal not affected by scalar coupling is at δ_H,δ_N 9.57,125.8 and is therefore assigned to M32.

Comparison of the chemical shift of M65, Table II, with the chemical shifts of the signals in the connectivity sequences, Table I, shows that M65 can be assigned to either a8 or c11. Taking the possible assignments of F61 and M65 together with the amino acid sequence, Figure 1, results in the unique set of assignments: a4, F61; a8, M65. The remaining assignments of the residues in the a sequence of d_{NN} connectivities, Table I, follow from the amino acid sequence, Figure 1. Three of the a sequence assignments (a2, S59; a9, V66; a10, E67) are confirmed by the proton shifts in Table II. In addition, we observe the splitting of the signal assigned to E67 (by [1-^{13}C]V66) in the HMQC spectrum (not shown) of Nase labeled with [1-^{13}C]V/[^{15}N]E. The expected splittings of E52 and E75 by V51 and V74 are also seen in the HMQC spectrum.

The assignments of the signals in the a sequence were obtained by assuming that one sequence of d_{NN} connectivities included amide proton signals of F61 and M65. Consideration of the proton chemical shifts in Tables I and II, together with the Nase amino acid sequence, shows that these remain the only tenable assignments if one assumes that one of the d_{NN} connectivities includes the amide proton signal of either F61 or M65.

Assignments of Signals in the b Sequence of d_{NN} Connectivities. The L103–V104 peptide bond occurs in the middle of the smallest helical domain of Nase, Figure 1. In order to assign the d_{NN} sequence containing signals of these residues, the chemical shifts of Val and Leu residues, Table II, were obtained from HMQC ^{1}H–^{15}N spectra, Figures 4 and 5, of the protein labeled with [1-^{13}C]L/[^{15}N]V and with [1-^{13}C]-K/[^{15}N]L/[^{15}N]S. In Figure 4, signals at δ_H 6.89 and 6.99 are split as a result of the L38-V39 and L103-V104 ^{13}C–^{15}N scalar couplings. The signal at δ_H 6.99 does not match the proton chemical shift of any signal in the d_{NN} connectivities, whereas the signal at δ_H 6.89 uniquely matches the chemical shift of b5. We therefore make the assignment of b5 to V104, because V104 is in a helical domain while V39 is not. This assignment implies that L103 must be assigned to either b4 or b6. A comparison of the proton chemical shifts of b4 and b6, Table I, with the amide proton shifts of Nase Leu residues, Table II, shows that b3 being L103 is the correct assignment. The assignments of the remaining signals in the b sequence of d_{NN} connectivities follow from the amino acid sequence. According to these assignments, b2 (δ_H 6.19) is E101 and b7 (δ_H 7.09) is Q106. These assignments were confirmed by the observation of signals having these proton chemical shifts in the HMQC spectrum of Nase containing [1-^{13}C]V/[^{15}N]-E/[^{15}N]Q, Table II.

Using the b sequence assignments, Table I, together with the chemical shifts in Table II, we can now extend the b sequence of d_{NN} connectivities originally identified in the NOESY spectra of Nase (Torchia et al., 1988) to include d_{NN} connectivities from three additional residues located at the N- and C-termini of the b sequence, i.e., V99, L108, and A109 having chemical shifts of δ_H 10.18, 7.79, and 6.92, respectively, as derived from the d_{NN} connectivities.

Assignments of Signals in the c Sequence of d_{NN} Connectivities. In order to assign the signals in the c sequence, we note that Nase contains a single K–S peptide bond, K127–S128, and that the HMQC spectrum of Nase containing [1-^{13}C]K/[^{15}N]L/[^{15}N]S, Figure 5, shows that a Ser signal having δ_H 7.58 is split. Hence, this signal is assigned to S128. Examination of Table I shows that either c4 or c11 can be assigned to S128. The latter assignment, according to the amino acid sequence, requires either that c4 be assigned to H121 or that c2 be assigned to L137. However, the chemical shift data in Tables I and II show that neither assignment is tenable, and this result implies that c4 must be assigned to S128. Of the 2 possible assignments of the 12 remaining signals in the c sequence, only the one listed in Table I is supported by the HMQC spectra. The alternative scheme

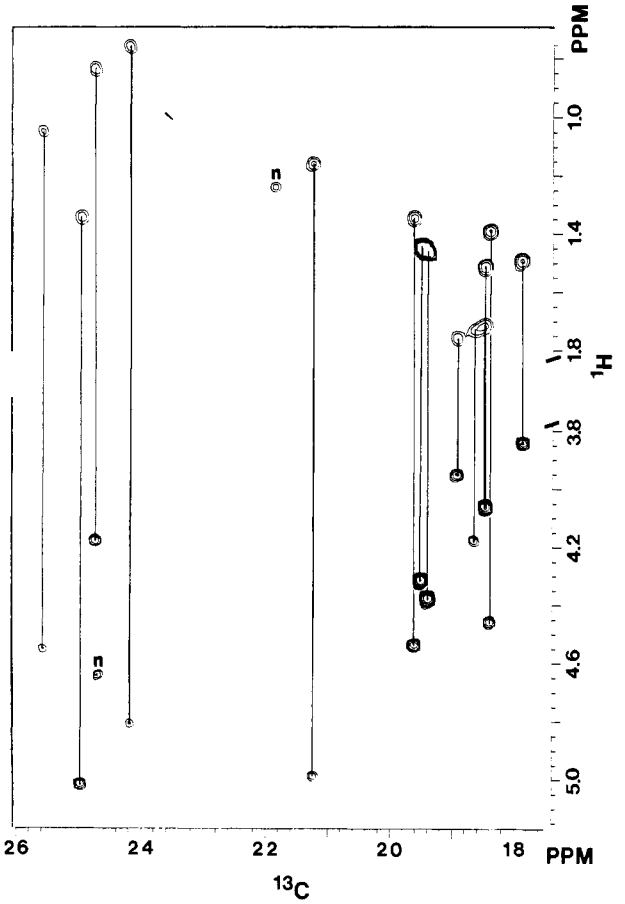

FIGURE 6: HMQC RELAY spectrum of Nase labeled with [3-^{13}C]A, showing the correlated α-proton and methyl proton signals of each of the 14 Ala residues in Nase. The weak uncorrelated signals, labeled n, are due to protons bonded to ^{13}C nuclei in natural abundance. Note the break in the proton chemical shift axis.

assigns c11 to H121, an assignment which is clearly incompatible with the H121 proton chemical shift listed in Table II. In contrast, the assignments listed in Table I (namely: c1, L125; c13, L137; c5, E129; c11 E135) are confirmed by the proton chemical shifts listed in Table II. In addition, the signal assigned to L137, δ_H 7.58, is split, Figure 5, by the K136-L137 scalar coupling. According to the amino acid sequence, the two other split Leu signals seen in Figure 5 are L7 and L25.

Assignments of Ala Signals in Sequences of d_{NN} Connectivities. We noted earlier that the level of ^{13}C enrichment was only 40–50% in the Nase sample labeled with [1-^{13}C]-A/[^{15}N]F. In addition, a proton spectrum of the deuteriated protein indicated that ca. 50% of the Ala residues were protonated at the α- and β- (methyl) positions. These observations suggested that it would be possible to identify the Ala $d_{\alpha\beta}(i,i)$ connectivities and correlate them with the $d_{\alpha N}(i,i)$ and $d_{\beta N}(i,i)$ connectivities of the seven Ala residues in the d_{NN} connectivity sequences. The homonuclear Hartmann–Hahn mechanism was used to correlate the α-proton and methyl proton chemical shifts, Table III, of the 14 Ala residues in the HMQC RELAY spectrum (Lerner & Bax, 1986) of Nase labeled with [3-^{13}C]Ala, Figure 6. An examination of the NOESY spectrum of deuteriated Nase, Figure 7, showed 11 $d_{\alpha\beta}(i,i)$ connectivities having proton chemical shifts, Table III, in excellent agreement with the shifts derived from the RELAY spectrum. Hence, these 11 connectivites are assigned to Ala residues. Because the NOESY spectrum was obtained in H_2O with solvent saturation, $d_{\alpha\beta}(i,i)$ connectivities were not observed for the three Ala residues that had α-proton chemical shifts within 0.15 ppm of the water signal.

Table III: Chemical Shifts and Assignments of Nase Ala α-Protons and Methyl Protons

$\delta_{H\alpha}{}^a$	$\delta_{H\beta}{}^a$	$\delta_{H\alpha}{}^b$	$\delta_{H\beta}{}^b$	assignment
4.81	0.77			
4.18	0.84	4.17	0.84	
4.55	1.05		1.04	A109
4.99	1.16	4.98	1.16	
5.01	1.35	4.99	1.33	
4.54	1.35		1.33	A69
4.46	1.40	4.44	1.41	
4.31	1.46	4.32	1.45	
4.38	1.46	4.33	1.47	
3.84	1.49	3.84	1.49	A130
4.06	1.52	4.05	1.52	A60
4.06	1.73	4.07	1.72	A102
4.17	1.73	4.16	1.74	A58
3.95	1.76	3.95	1.76	A132

[a] From ^{1}H–^{13}C HMQC spectrum, Figure 6. [b] From NOESY spectrum, Figure 7.

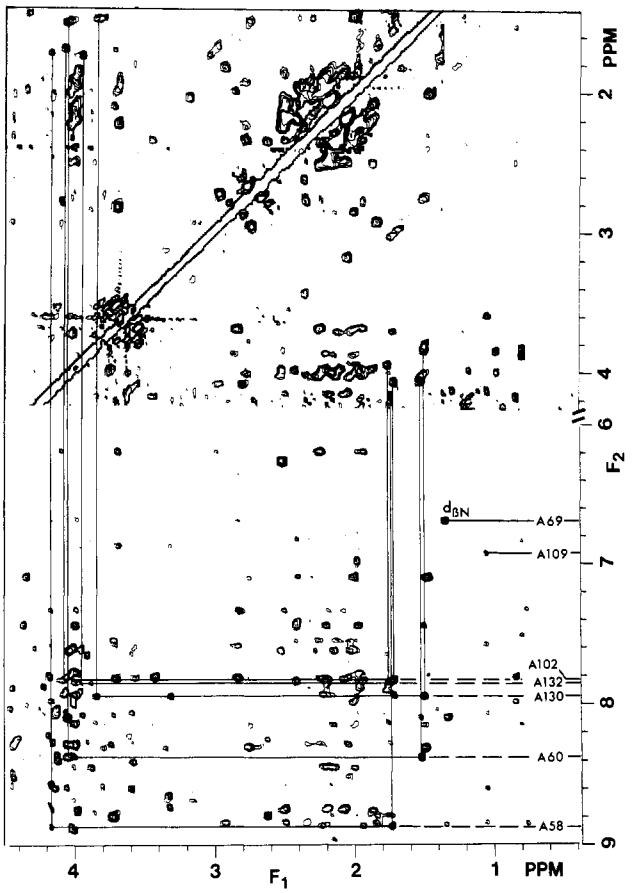

FIGURE 7: Portion of the NOESY spectrum of deuteriated Nase. Each of the three-segment solid lines correlates the $d_{\alpha\beta}(i,i)$, $d_{\alpha N}(i,i)$, and $d_{\beta N}(i,i)$ connectivites of one of the Ala residues assigned to the d_{NN} connectivity sequences. The terminal points of each line are at the Ala $d_{\alpha\beta}(i,i)$ connectivities, and the break points are at the Ala $d_{\alpha N}(i,i)$ and $d_{\beta N}(i,i)$ connectivities. The $d_{N\beta}(i,i)$ connectivities of A 69 and A109 are indicated by the labeled horizontal lines. The amide proton chemical shifts of the Ala residues in the d_{NN} sequences are given on the vertical axis. Note the break in this axis between 4 and 6 ppm.

The chemical shifts in Tables I and II enable one to locate sets of Ala $d_{\alpha\beta}(i,i)$, $d_{\alpha N}(i,i)$, and $d_{\beta N}(i,i)$ connectivites in the NOESY spectrum, Figure 7, for five of the seven Ala residues in the d_{NN} sequences. The A69 and A109 $d_{\alpha N}(i,i)$ connectivities are not seen in Figure 7. However, the $d_{\beta N}(i,i)$ connectivities are observed and show that $\delta_{H\beta}$ 1.35 and 1.04 are for A69 and A109, respectively. This result and the shift correlations listed in Table III show that $\delta_{H\alpha}$ 4.54 and 4.55

are for A69 and A109, respectively. The proximity of the A69 and A109 α-proton signals to the water signal explains the absence of the A69 and A109 $d_{\alpha N}(i,i)$ connectivities. These results obtained from the NOESY and RELAY spectra not only confirm the assignments in Table I but also provide assignments for all protons of the seven Ala residues in the helical domains of Nase.

The availability of the helical Ala α-proton assignments enabled us to examine the NOESY spectrum of deuteriated Nase for $d_{\alpha N}(i,i+3)$ connectivities. These connectivites are expected to be weak because $d_{\alpha N}(i,i+3)$ is 3.4 Å in an α-helix (Wuethrich, 1986) and because the Ala α-positions are ca. 50% deuteriated. Nevertheless, connectivites were found for A102–R105, A130–K133, and A132–E135 in the NOESY spectrum obtained with a 300-ms mixing time. Connectivities involving A58–F61 and A60–K63 could not be conclusively identified because they were obscured by overlaps with intense cross-peaks.

Discussion

Sequential assignments of the amide proton signals in the three helical domains of Nase have been made by comparing chemical shifts derived from the enhanced d_{NN} connectivities observed in the NOESY spectrum of the deuteriated protein with shifts observed in the heteronuclear edited HMQC spectra of the $^{15}N/^{13}C$-labeled protein. This approach differs from the standard method of sequential assignments (Wuethrich, 1986) and is most useful for assigning amide proton signals in the helical domains of proteins that are too large to apply the standard approach. When a crystal structure is not available, a predictive algorithm can be used to identify amino acid residues most suitable for labeling, i.e., those likely to be in helical domains.

A noteworthy feature of our approach is that it has been successfully applied to a protein having a M_r of 18K, at low concentration and at physiological temperature, ionic strength, and pH. Although extensive labeling is required, the use of an efficient expression system greatly reduces the labor and expense of the sample preparations. Because of the high sensitivity and resolution of the HMQC experiment when applied to a labeled sample, spectra are typically obtained in a few hours, even at the low protein concentration used herein, and chemical shifts of both the heteronucleus and its bonded proton are obtained for all labeled amino acid residues in the protein.

Figure 1 shows that the signals connected by the d_{NN} sequences correspond, almost exclusively, to the hydrogen-bonded amide protons in the Nase α-helices, suggesting a close correspondence between the solution and crystal structures of the protein. However, the values of d_{NN} calculated from the X-ray structure are in the range 2.02–3.59 Å, for residues 60–69. In contrast, the variation in the buildup rates of the corresponding d_{NN} connectivities is at most threefold, implying that the values of d_{NN} vary by less than ±12%. The discrepancy between the X-ray and NMR results may arise from a difference between the solid-state and solution structures of Nase but may also reflect experimental uncertainties in the values of d_{NN}.

The amide proton assignments listed in Table I can be used to examine how a myriad of interesting variables affect the α-helical domains of Nase. In addition, the assignments of the nonhelical amide signals, Table II, provide important starting points for working out sequences of $d_{\alpha N}$ and $d_{\alpha N}(i,i)$ connectivities. These connectivity sequences will provide assignments and structural information about residues in β-strands in Nase and thereby pave the way for studies of these important structural domains in the protein.

Added in Proof

After this paper was accepted for publication, a new set of refined X-ray coordinates of crystalline Nase/pdTp/Ca^{2+} was made available to us (Professor E. Lattman and Dr. P. Loll, private communication). The values of the d_{NN} derived from these coordinates vary by less than ±13%, for residues 60–69, in agreement with the NOESY data.

Acknowledgments

We thank Professor John Gerlt for providing us with the transformed *E. coli* used to make Nase and Rolf Tschudin for expert technical support.

References

Bax, A., Griffey, R. H., & Hawkins, B. L. (1983) *J. Magn. Reson. 55*, 301–315.
Bendall, M. R., Pegg, D. T., & Dodrell, D. M. (1983) *J. Magn. Reson. 52*, 81–117.
Calderon, R. O., Stolowich, N. J., Gerlt, J. A., & Sturtevant, J. M. (1985) *Biochemistry 24*, 6044–6049.
Clore, G. M., Gronenborn, A. M., Brunger, A. T., & Karplus, M. (1985) *J. Mol. Biol. 186*, 435–455.
Cross, T. A., & Opella, S. J. (1985) *J. Mol. Biol. 182*, 367–381.
Evans, P. A., Dobson, C. M., Kautz, R. A., Hatfull, G., & Fox, R. O. (1987) *Nature (London) 329*, 266–270.
Fox, R. O., Evans, P. A., & Dobson, C. M. (1986) *Nature (London) 320*, 192–194.
Griffey, R. H., & Redfield, A. G. (1987) *Q. Rev. Biophys. 19*, 51–82.
Griffey, R. H., Redfield, A. G., Loomis, R. E., & Dahlquist, F. W. (1985) *Biochemistry 24*, 817–822.
Griffey, R. H., Redfield, A. G., McIntosh, L. P., Oas, T. G., & Dahlquist, F. W. (1986) *J. Am. Chem. Soc. 108*, 6816–6817.
Hibler, D. W., Stolowich, N. J., Reynolds, M. A., Gerlt, J. A., Wilde, J. A., & Bolton, P. H. (1987) *Biochemistry 26*, 6278–6286.
Kainosho, M., & Tsuji, T. (1982) *Biochemistry 21*, 6273–6279.
Klevit, R. E., & Drobny, G. P. (1986) *Biochemistry 25*, 7760–7769.
Leighton, P., & Lu, P. (1987) *Biochemistry 26*, 7262–7271.
LeMaster, D. M., & Richards, F. M. (1988) *Biochemistry 27*, 142–150.
Lerner, L., & Bax, A. (1986) *J. Magn. Reson. 69*, 375–380.
McIntosh, L. P., Griffey, R. H., Muchmore, D. C., Nielson, C. P., Redfield, A. G., & Dahlquist, F. W. (1987) *Proc. Natl. Acad. Sci. U.S.A. 84*, 1244–1248.
McIntosh, L. P., Dahlquist, F. W., & Redfield, A. G. (1988) *J. Biomol. Struct. Dyn. 5*, 21–34.
Mueller, L. (1979) *J. Am. Chem. Soc. 101*, 4481–4484.
Redfield, A. G. (1983) *Chem. Phys. Lett. 96*, 537–540.
Senn, H., Otting, G., & Wuethrich, K. (1987) *J. Am. Chem. Soc. 109*, 1090–1092.
Serpersu, E. H., Shortle, D., & Mildvan, A. S. (1987) *Biochemistry 26*, 1289–1300.
Shortle, D. (1983) *Gene 22*, 181–189.
Shortle, D., & Lin, B. (1985) *Genetics 111*, 539–555.
Sklenar, V., & Bax, A. (1987) *J. Magn. Reson. 74*, 469–479.
Torchia, D. A., Sparks, S. W., & Bax, A. (1988) *J. Am. Chem. Soc 110*, 2320–2321.
Tucker, P. W., Hazen, E. E., & Cotton, F. A. (1978) *Mol. Cell. Biol. 22*, 67–77.

Tucker, P. W., Hazen, E. E., & Cotton, F. A. (1979a) *Mol. Cell. Biol. 23*, 3–16.
Tucker, P. W., Hazen, E. E., & Cotton, F. A. (1979b) *Mol. Cell. Biol. 23*, 67–86.
Tucker, P. W., Hazen, E. E., & Cotton, F. A. (1979c) *Mol. Cell. Biol. 23*, 131–141.
Wand, A. J., & Englander, S. W. (1985) *Biochemistry 24*, 5290–5294.
Weber, P. L., Wemmer, D. E., & Reid, B. R. (1985) *Biochemistry 24*, 4553–4562.
Williamson, M. P., Marion, D., & Wuethrich, K. (1984) *J. Mol. Biol. 173*, 341–359.
Wuethrich, K. (1986) *NMR of Proteins and Nucleic Acids*, Wiley, New York.
Zuiderweg, E. R. P., Kaptein, R., & Wuethrich, K. (1983) *Proc. Natl. Acad. Sci. U.S.A. 80*, 5837–5841.

Mapping of the Nucleotide-Binding Sites in the ADP/ATP Carrier of Beef Heart Mitochondria by Photolabeling with 2-Azido[α-^{32}P]adenosine Diphosphate†

Pascal Dalbon,‡ Gérard Brandolin,‡ François Boulay,‡ Jürgen Hoppe,§ and Pierre V. Vignais‡

Laboratoire de Biochimie, Département de Recherche Fondamentale, Centre d'Etudes Nucléaires, 85X, 38041 Grenoble Cedex, France, and Institut für Physiologische Chemie, Universität Würzburg, Koellickerstrasse 2, D-8700 Würzburg, FRG

Received December 15, 1987; Revised Manuscript Received February 16, 1988

ABSTRACT: 2-Azido[α-^{32}P]adenosine diphosphate (2-azido[α-^{32}P]ADP) has been used to photolabel the ADP/ATP carrier in beef heart mitochondria. In reversible binding assays carried out in the dark, this photoprobe was found to inhibit ADP/ATP transport in beef heart mitochondria and to bind to two types of specific sites of the ADP/ATP carrier characterized by high-affinity binding (K_d = 20 μM) and low-affinity binding (K_d = 400 μM). In contrast, it was unable to bind to specific carrier sites in inverted submitochondrial particles. Upon photoirradiation of beef heart mitochondria in the presence of 2-azido[α-^{32}P]ADP, the ADP/ATP carrier was covalently labeled. After purification, the photolabeled carrier protein was cleaved chemically by acidolysis or cyanogen bromide and enzymatically with the *Staphylococcus aureus* V8 protease. In the ADP/ATP carrier protein, which is 297 amino acid residues in length, two discrete regions extending from Phe-153 to Met-200 and from Tyr-250 to Met-281 were labeled by 2-azido[α-^{32}P]ADP. The peptide fragments corresponding to these regions were sequenced, and the labeled amino acids were identified. As 2-azido-ADP is not transported into mitochondria and competes against transport of externally added ADP, it is concluded that the two regions of the carrier which are photolabeled are facing the cytosol. Whether the two photolabeled regions are located in a single peptide chain of the carrier or in different peptide chains of an oligomeric structure is discussed.

The mitochondrial ADP/ATP carrier is characterized by specific binding sites for the free forms of the natural substrates ADP and ATP. Two conformers of the ADP/ATP carrier exist, which can be differentiated by the binding of two categories of specific inhibitors, namely, atractyloside (ATR)[1] and carboxyatractyloside (CATR), on one hand, and bongkrekic and isobongkrekic acids (BA and isoBA) on the other [for review cf. Vignais et al. (1985)]. The ADP/ATP carrier molecule also contains amino acid residues whose modification results in inactivation of transport (Block et al., 1981). The beef heart ADP/ATP carrier is a protein of 297 amino acid residues whose sequence has been reported (Aquila et al., 1982). In this carier, a sequence has been identified, which spans residues Cys-159–Met-200 and is involved in ATR (CATR) binding (Boulay et al., 1983). Furthermore, the strategic cysteinyl residue that becomes exposed at the onset of transport and whose alkylation by *N*-ethylmaleimide inhibits the functioning of the carrier and prevents ATR binding, but not BA binding, has been assigned to position 56 (Boulay & Vignais, 1984). Mapping of the nucleotide-binding site(s) of the ADP/ATP carrier has not been reported so far. Such mapping requires the use of a photoprobe able to bind with high affinity and specificity to the carrier protein. Preliminary studies have shown that 2-azido[α-^{32}P]ADP binds reversibly and with high affinity to the ADP/ATP carrier in rat heart mitochondria in the absence of photoirradiation and competitively inhibits ADP transport (Dalbon et al., 1985). The ADP/ATP carrier from beef heart mitochondria can be prepared in large amounts, and a number of mapping studies have been conducted with this carrier (see above); for these reasons, we decided to use the beef heart mitochondrial ADP/ATP carrier for photolabeling studies. This paper describes the reactivity of 2-azido[α-^{32}P]ADP toward the ADP/ATP carrier in beef heart mitochondria and inverted

† This work was supported by grants from the Centre National de la Recherche Scientifique (CNRS/UA 1130), the Institut National de la Santé et de la Recherche Médicale, and the Université Scientifique Technologique et Médicale de Grenoble, Faculté de Médecine.

‡ Centre d'Etudes Nucléaires.
§ Universität Wurzburg.

[1] Abbreviations: ATR, atractyloside; CATR, carboxyatractyloside; BA, bongkrekic acid; 2-azido-ADP, 2-azidoadenosine diphosphate; DITC, *p*-phenylene diisothiocyanate; PTH, phenylthiohydantoin; HEPES, 4-(2-hydroxyethyl)-1-piperazineethanesulfonic acid; γ-AmNS-ATP, adenosine N^{γ}-(5-sulfo-1-naphthyl)triphosphoramidate; NEM, *N*-ethylmaleimide; NAP_4ATR, 4-azido-2-nitrophenyl aminobutyryl-ATR; Hse, homoserine lactone; EDTA, ethylenediaminetetraacetic acid; MOPS, 4-morpholinepropanesulfonic acid; Tris, tris(hydroxymethyl)-aminomethane; $NaDodSO_4$, sodium dodecyl sulfate.

0006-2960/88/0427-5141$01.50/0